MIT Open Access Articles

Position-Dependent Silencing of Germline V beta Segments on TCR beta Alleles Containing Preassembled V beta DJ beta C beta 1 Genes

Position Dependent Silencing of Germline Vβ Segments on TCRβ Alleles Containing Pre-Assembled VβDJβCβ1 Genes

Brenna L. Brady[*,†], **Michael A. Oropallo**[*], **Katherine S. Yang-Iott**[†], **Thomas Serwold**[‡], **Konrad Hochedlinger**[§], **Rudolf Jaenisch**[¶], **Irving L. Weissman**[‡], and **Craig H. Bassing**[*,†,‖]

[*] Immunology Graduate Group, University of Pennsylvania School of Medicine, Philadelphia, PA 19104

[†] Division of Cancer Pathobiology, Department of Pathology and Laboratory Medicine, Center for Childhood Cancer Research, Children's Hospital of Philadelphia, Abramson Family Cancer Research Institute, University of Pennsylvania School of Medicine, Philadelphia, PA 19104; USA

[‡] Harvard Medical School, Joslin Diabetes Center, Room 468A, 1 Joslin Place, Boston, MA 02115; USA

[§] Department of Medicine, Harvard Medical School, Massachusetts General Hospital, Cancer Center and Center for Regenerative Medicine, Boston, MA 02114; USA

[¶] Whitehead Institute for Biomedical Research, Massachusetts Institute of Technology, Cambridge, MA 02142; USA

Abstract

The genomic organization of TCRβ loci enables Vβ-to-DJβ2 rearrangements on alleles with assembled VβDJβCβ1 genes, which could have deleterious physiologic consequences. To determine whether such Vβ rearrangements occur and if so how they might be regulated, we analyzed mice with TCRβ alleles containing pre-assembled functional VβDJβCβ1 genes. Vβ10 segments were transcribed, rearranged, and expressed in thymocytes when located immediately upstream of a Vβ1DJβCβ1 gene, but not on alleles with a Vβ14DJβCβ1 gene. Germline Vβ10 transcription was silenced in mature αβ T cells. This allele-dependent and developmental stage-specific silencing of Vβ10 correlated with increased CpG methylation and decreased histone acetylation over the Vβ10 promoter and coding region. Transcription, rearrangement, and expression of the Vβ4 and Vβ16 segments located upstream of Vβ10 were silenced on alleles containing either VβDJβCβ1 gene; sequences within Vβ4, Vβ16, and the Vβ4/Vβ16--Vβ10 intergenic region exhibited constitutive high CpG methylation and low histone acetylation. Collectively, our data indicate that the position of Vβ segments relative to assembled VβDJβCβ1 genes influences their rearrangement and suggest that DNA sequences between Vβ segments may form boundaries between active and inactive Vβ chromatin domains upstream of VβDJβCβ genes.

Introduction

In humans and mice, αβ T lymphocytes are generated through a step-wise differentiation program that requires the assembly and expression of functional T cell receptor (TCR) genes to progress through developmental checkpoints (1). In CD4⁻CD8⁻ (double negative, or DN) thymocytes, TCRβ genes are assembled in a temporal manner with Dβ-to-Jβ recombination

[‖]Corresponding Author: Craig H. Bassing, Ph.D. 4054 Colket Translational Research Building, Children's Hospital of Philadelphia, 3501 Civic Center Blvd. Philadelphia, PA 19104, Phone: 267-426-0311, FAX: 267-426-2791, bassing@email.chop.edu.

initiating before Vβ rearrangements, which occur to DJβ complexes on one allele at a time (2). TCRβ chains encoded by in-frame VβDJβ rearrangements can pair with pTα molecules to form pre-TCRs that rescue DN cells from death and signal proliferation and differentiation into CD4$^+$CD8$^+$ (double positive, or DP) thymocytes (1). TCRβ/pTα-dependent signals also inhibit Vβ rearrangements on the other allele to suppress development of cells with TCRβ chains expressed from both alleles (1,2). If an out-of-frame TCRβ gene is assembled on the first allele, TCRβ/pTα-mediated feedback inhibition is not signaled and Vβ rearrangements can initiate on the other allele (2). In DP thymocytes, TCRβ rearrangements remain suppressed while TCRα genes are assembled through bi-allelic Vα-to-Jα rearrangements (2). TCRα chains encoded by in-frame VαJα rearrangements may pair with TCRβ chains to form αβ TCR (1). Upon their positive selection, αβ TCRs rescue DP cells from death and signal differentiation into CD4$^+$ or CD8$^+$ (single positive, SP) thymocytes, which migrate into the periphery as αβ T cells (1). However, DP thymocytes expressing auto-reactive αβ TCRs can be eliminated by apoptosis to help preserve self-tolerance (1).

The mouse and human TCRβ loci each contain a cluster of ~33 Vβ segments and two Dβ-Jβ-Cβ clusters (3). Both loci contain the Vβ14 segment outside of the Vβ cluster, while the mouse locus also contains a Vβ2 segment far upstream of the Vβ cluster. On any individual TCRβ allele, the Dβ1 segment can recombine with Jβ1 or Jβ2 segments, the Dβ2 segment can recombine with Jβ2 segments; any Vβ segment can rearrange to an assembled Dβ1Jβ1, Dβ1Jβ2, or Dβ2Jβ2 complex. In mouse αβ T cells, DJβ1 and DJβ2 complexes are equally represented in VβDJβ rearrangements on both selected and non-selected alleles (4). These data suggest that Vβ-to-DJβ2 rearrangements over assembled VβDJβ1Cβ1 genes are suppressed by active mechanisms. Such secondary Vβ rearrangements would have deleterious immunological consequences regardless of whether the VβDJβ1Cβ1 genes had been assembled in-frame or out-of-frame. Since approximately two-thirds of VβDJβ exons are assembled out-of-frame, most Vβ-to-DJβ2 rearrangements on alleles with in-frame VβDJβ1 exons would be wasteful and decrease the overall efficiency at which functional TCRβ genes are formed. Alternatively, the assembly of in-frame Vβ-to-DJβ2 rearrangements on alleles with functional VβDJβ1Cβ1 genes could occur during αβ TCR selection and replace a self-tolerant receptor with an auto-reactive one. In cells with TCRβ chains expressed from the other allele, in-frame Vβ-to-DJβ2 rearrangements on alleles with non-functional VβDJβ1Cβ1 genes would result in TCRβ allelic inclusion that could short-circuit negative selection and lead to development of auto-reactive αβ T cells.

The mechanisms by which TCRβ chains are assembled and expressed from a single allele in the majority of thymocytes remain speculative, but likely involve epigenetic regulation of Vβ chromatin structure and changes in topology and nuclear localization of TCRβ loci. Active Vβ rearrangement in DN cells correlates with germline Vβ transcription, hyper-acetylated and nuclease accessible Vβ (and Dβ-Jβ) chromatin, and TCRβ locus contraction by looping between Vβ and Dβ/Jβ segments (5–7). Suppression of Vβ rearrangement in DP thymocytes correlates with decreased Vβ transcription, down-regulation of Vβ chromatin histone acetylation and nuclease accessibility, and de-contraction of TCRβ loci (5–8). These analyses of germline Vβ segments in DP cells have been conducted on sorted DP or total thymocytes isolated from RAG-deficient thymocytes treated with anti-CD3 antibodies or expressing a TCRβ transgene (6,7,9,10). Anti-CD3 antibodies and TCRβ transgenes both induce DN-to-DP differentiation in the absence of TCRβ rearrangements, but germline Vβ transcription and histone modifications in Vβ chromatin are not down-regulated to the same extent in DP cells induced by anti-CD3 antibodies (9,10), which raises questions regarding the physiologic relevance of these studies (11). Germline Vβ segments upstream of assembled VβDJβCβ genes can reside within open chromatin structures and be transcribed in peripheral αβ T cells (11), however similar experiments in DP thymocytes have not been

reported. Therefore, to identify potential mechanisms that suppress Vβ-to-DJβ2 rearrangements over VβDJβ1Cβ1 genes, we characterized the expression, chromatin structure, and rearrangement of germline Vβ segments on alleles containing pre-assembled functional VβDJβCβ1 genes.

Materials and Methods

Mice

Generation and characterization of Vβ1$^{NT/+}$ (LN3β) mice and LN2 embryonic stem cells containing the pre-assembled Vβ14Dβ1Jβ1.4Cβ gene were previously described (12,13). Vβ1$^{NT/+}$ mice were bred onto a 129SvEv (Taconic) background and mated with one another to generate the Vβ1$^{NT/+}$, Vβ1$^{NT/NT}$, and wild-type mice used in experiments. LN2 cells were used to generate mice with the Vβ14^{NT} allele transmitted through the germline. These mice were mated with 129SvEv mice to isolate the Vβ14^{NT} allele from the other rearranged TCRβ and TCRα alleles. Both Vβ1$^{NT/NT}$ and Vβ14$^{NT/NT}$ mice were bred with C57BL6 Rag1$^{-/-}$ mice (Jackson Laboratories) and offspring bred together to generate the Vβ1$^{NT/+}$Rag1$^{-/-}$, Vβ1$^{NT/NT}$Rag1$^{-/-}$, Vβ14$^{NT/+}$Rag1$^{-/-}$, and Vβ14$^{NT/NT}$Rag1$^{-/-}$ mice. All experiments in mice were performed in accordance relevant institutional and national guidelines and regulations and approved by the Children's Hospital of Philadelphia IACUC committee.

Flow cytometry

Single cell suspensions of thymocytes or splenocytes were incubated with red blood cell lysis buffer (0.7 M NaCl and 17 mM Tris HCl). Cells were stained with antibodies in PBS containing 1% BSA and 1mM EDTA. Antibodies were purchased from BD Pharmigen: anti-Vβ4 (553364), anti-Vβ8 (553862), anti-Vβ10 (553285), anti-Vβ14 (553258), anti-CD4 (553051), anti-CD8α (553033), anti-Cβ (553174), anti-CD25(552880), and anti-CD117 (553356). FACS plots were gated on live lymphocytes determined by propidium iodide exclusion and forward and side scatter. DN stains were gated on lineage negative cells using a lineage cocktail of the following antibodies: anti-TCRβ (553172), anti-B220 (553090), anit-CD19 (553786), anti-CD11b (553311), anti-CD11c (557401), anti-C^{TM} (553178), anti-NK1.1 (553165), anti-CD8α (553033), and anti-Ter119 (553673). Analysis was preformed on a FACS caliber and data analysis was preformed with FlowJo.

PCR Analysis of Vβ Rearrangements

Genomic DNA was isolated from total thymus using lysis buffer (0.1 M Tris pH 8.5, 0.2% SDS, 0.005 M EDTA, 0.2 M NaCl, and 250μg/μl Proteinase K) and quantified by spectrophotometer. PCR primer sequences are listed in Supplemental Table 1. PCR conditions for a final volume of 25μL were 10 X PCR Buffer (Qiagen), 0.2 mM dNTPs (ABI), 0.2 mM each primer, 5 units of Hot Star Taq polymerase (Qiagen), and 500 ng DNA. PCR cycles were: 94°C for 3 minutes; 40 cycles of 94°C for 45 seconds, 60°C for 1:30 minutes, 72°C for 2:30 minutes; and 72°C for 10 minutes.

Generation and Analysis of Hybridomas

The generation and analysis of TCRβ gene rearrangements Vβ1$^{NT/+}$ and Vβ1$^{NT/NT}$αβ T cell hybridomas were conducted exactly as described previously (4,14).

Real-time PCR for Transcripts

RNA was isolated from 10 million cells using Tri-reagent. Genomic DNA was digested with 2 units RQ1 DNase (Promega) with the required buffers. cDNA was synthesized with the NEB protoscript II kit and gene specific primers. cDNA was synthesized with three primers

per reaction used at a final concentration of 0.175 mM each. Combinations of primers (See Supplemental Table 1) were as follows, with sense and anti-sense reactions carried out separately: Vβ1, Vβ10, and 18s RNA; Vβ4, Vβ18, and 18s RNA; Vβ14, Vβ16, and 18s RNA. Real-time PCR conditions for a final volume of 15 μL were 2X SYBR Green Master Mix (ABI), 0.667 mM final concentration of each primer, and 1 μL of DNA or RNA. Controls without reverse-transcriptase (RT) enzyme were analyzed for each RT reaction. Transcripts were normalized to the level of 18s RNA. PCR cycles were: 50°C for 2 minutes; 95°C for 10 minutes; 40 cycles of 95°C for 15 seconds, 60°C for 1 minute. Dissociate curves were run to assure a single product.

Enrichment of Splenic αβ T cells

The enrichment of αβ T cells from total splenocytes was conducted using BioMag goat anti-rat IgG magnetic beads (Qiagen). Splenic single cell suspensions were incubated with 1μg anti-CD4 and 1μg anti-CD8α (BD pharmigen). Cell/antibody complexes were incubated with 2.5 mL of magnetic beads and applied to a magnet. Cell bead complexes were then used for either RNA or DNA isolation as described above.

Methyl Sensitive Restriction Assay

DNA was prepared from whole thymuses and digested with EcoRI. Digests were phenol chlorophorm extracted and quantified. 2 μ of DNA was digested with HincII, AvaI, BstUI, HpaII, or HaeII (NEB) in respective buffers with 1X BSA; undigested controls without enzyme were included. Samples were phenol chloroform extracted and re-suspended in 30 μL water. Percent methylation was quantified by real-time PCR. Real-time PCR conditions for a final volume of 15 μL were 2X SYBR Green Master Mix (ABI), 0.667 mM final concentration each primer, and 1 μL of DNA. DNA content was assayed by amplification with the methyl quant F and R primer set (Supplemental Table 1) whose amplicon does not contain any of the above restriction sites. Digested and undigested samples were normalized to this primer set and percent methylation was determined by dividing digested by undigested samples.

Chromatin Immunoprecipitation

Mononucleosomes were prepared from 1×10^7 thymocyes or splenic T cells of 4–6 week old mice. Cells were lysed in 100 μL cell lysis buffer (80 mM NaCl, 10 mM Tris-HCl pH 7.5, 10 mM sodium butyrate, 6 mM MgCl2, 1 mM CaCl$_2$, 250 mM sucrose, 0.1 mM PMSF, and 0.1 mM benzamidine) and 100μL buffer containing 0.04% (v/v) NP-40 for 5 minutes on ice. Nuclei were washed with 200 μL digestion buffer (10 mM NaCl, 10 mM Tris-HCl pH 7.5, 10 mM sodium butyrate, 3 mM MgCl2, 1 mM CaCl$_2$, and 250 mM sucrose). Mononucleosomes were obtained through incubation of nuclei with 1 Unit micrococcal nuclease (Worthington) in digestion buffer for 5 minutes at 37°C followed by sonication. Chromatin was incubated overnight with either anti-Acetyl-H3 (Millipore 07-593), anti-Acetyl H4 (Upstate 06-866), or control rabbit IgG (Sigma 18140-10MG). Immune complexes were precipitated with protein A beads (Millipore 16-157). DNA was isolated and subjected to real-time PCR analysis as above.

Bisulfite Sequencing

Genomic DNA was mutated with Imprint® DNA Modification Kit (Sigma). Mutated DNA was amplified by PCR using the primers Vβ10BisF: 5′-GGTTAGGAGATATGATTTGTTT-3′ and Vβ10BisR: 5′-CAATTAAAAAACACTTCATTTCCC-3′. PCR products were subcloned and sequenced.

Results

Expression of Vβ10 Segments from Endogenous TCRβ Alleles containing a Pre-assembled In-Frame Vβ1DJβ1.4Cβ1 Gene

Nuclei of αβ T cells have been used in nuclear transfer (NT) experiments to establish mice containing a pre-assembled in-frame endogenous Vβ1DJβ1.4 rearrangement on one allele (hereafter referred to as the Vβ1^{NT} allele) and a wild-type germline TCRβ locus on the other allele (Vβ1$^{NT/+}$ mice)(13). Vβ1$^{NT/+}$ mice have previously been shown to exhibit grossly normal αβ T cell development, with the only exceptions being decreased numbers of DN thymocytes and an altered ratio of CD4$^+$ and CD8$^+$ cells due to expression of the pre-assembled TCRβ gene (12). The TCRβ locus of the Vβ1^{NT} allele contains deletion of sequences between Vβ1 and Jβ1.4, a germline Dβ2-Jβ2 cluster, and five germline Vβ segments (Figure 1a). Vβ10 resides immediately upstream of the pre-assembled Vβ1DJβ1.4 exon. Vβ4 and Vβ16 segments reside within a Vβ sub-cluster that is separated from Vβ10 by 13.5 kb of intergenic sequences that contain multiple transposons and other repetitive DNA elements. Vβ2 and Vβ14 are located outside of the Vβ cluster. In thymocytes, Dβ2-to-Jβ2 rearrangements and Vβ-to-DJβ2 recombination events involving Vβ2, Vβ14, Vβ4, Vβ16, and Vβ14 are each possible on the Vβ1^{NT} allele. Consequently, mice containing the Vβ1^{NT} allele provide a useful experimental model to evaluate whether regulation of Vβ chromatin might suppress Vβ-to-DJβ2 rearrangements over VβDJβ1Cβ1 genes,

We reasoned that mice containing the pre-assembled Vβ1DJβ1.4Cβ1 gene within both endogenous TCRβ alleles would facilitate investigation of molecular events involving germline Vβ segments on Vβ1^{NT} alleles. Thus, we bred together Vβ1$^{NT/+}$ mice to establish and analyze littermate or age-matched 4–6 week old Vβ1$^{NT/+}$, Vβ1$^{NT/NT}$, and wild-type (WT) mice. Cell counting and flow cytometric (FACS) analysis of thymocytes and splenocytes with anti-CD4 and anti-CD8 antibodies revealed that Vβ1$^{NT/NT}$ mice exhibit grossly normal αβ T cell development, with the only exception being an altered ratio of CD4$^+$ and CD8$^+$ cells similar to Vβ1$^{NT/+}$ mice (data not shown). In DN thymocytes, Dβ-to-Jβ rearrangements are detectable in ckit$^+$CD25$^+$ (DNI) cells (15), while Vβ-to-DJβ recombination events initiate in CD44$^+$(ckit$^+$)CD25$^+$ (DNIII) cells and, if functional, promote differentiation into CD44$^-$(ckit$^-$)CD25$^-$ (DNIV) cells (16). Cell counting and FACS analysis of CD4$^-$CD8$^-$ thymocytes with anti-ckit and anti-CD25 antibodies revealed that Vβ1$^{NT/+}$ and Vβ1$^{NT/NT}$ mice each contained fewer percentages of DNIII thymocytes, as compared to WT mice (Figure 1b). Notably, DNIII cell percentages were equivalently reduced in Vβ1$^{NT/NT}$ and Vβ1$^{NT/+}$ mice (Figure 1b), revealing that the presence of a functional endogenous Vβ1DJβ1.4Cβ1 gene on one or two alleles results in an indistinguishable acceleration of early thymocyte development.

We next conducted FACS analysis of Vβ1$^{NT/NT}$, Vβ1$^{NT/+}$, and WT lymphocytes with an anti-Cβ antibody and anti-Vβ antibodies specific for particular Vβ segments. The Vβ1^{NT} allele can express TCRβ chains containing Vβ1 or possibly one of the five remaining germline Vβ segments (Vβ2, Vβ4, Vβ16, Vβ10, and Vβ14). Unfortunately, FACS analyses of potential Vβ1 or Vβ16 expression and TCRβ allelic inclusion involving Vβ1 are not possible since anti-Vβ1 and anti-Vβ16 antibodies are not available. We observed dramatically lower percentages of cells expressing Vβ4, Vβ10, Vβ8, or Vβ14 on thymocytes and splenocytes isolated from Vβ1$^{NT/NT}$ and Vβ1$^{NT/+}$ mice, as compared to WT mice (Figure 2a,b,c). However, the percentages of cells expressing Vβ10 were not reduced to the same extent as the percentages of cells expressing Vβ4, Vβ8, or Vβ14. These data reveal that Vβ10 is the predominant Vβ segment expressed from the Vβ1^{NT} allele. We did not find expression of Vβ10 on αβ T lineage cells isolated from mice containing a pre-assembled in-frame endogenous Vβ14DJβ1.4Cβ1 gene on one allele and a wild-type germline TCRβ locus on the other allele (Vβ14$^{NT/+}$ mice, (17)). Critically, these data indicate that Vβ10

expression within TCRβ chains on Vβ1^NT/+ and Vβ1^NT/NT cells is dependent upon the Vβ1^NT allele, rather than ineffective silencing of Vβ10DJβ rearrangements on the wild-type allele due to accelerated early thymocyte development.

Frequent Vβ10-to-DJβ2 Rearrangements on Vβ1^NT Alleles

The significantly greater expression of Vβ10, as compared to Vβ4 or Vβ14, within cell surface TCRβ chains on Vβ1^NT/NTαβ T lineage cells could be due to differences in regulation of Vβ rearrangements to DJβ2 complexes, silencing of in-frame VβDJβ2 rearrangements, or pairing of VβDJβ2 chains with TCRα chains. To determine the relative frequencies at which germline Vβ segments rearrange to DJβ2 complexes on the Vβ1^NT allele, we conducted PCR analysis of Vβ-to-DJβ rearrangements using a primer specific for the Vβ4, Vβ8, Vβ10, or Vβ14 segment and a primer that anneals downstream of the Jβ1.2 or Jβ2.2 segment (Figure 3a). We amplified potential VβDJβ1 and VβDJβ2 rearrangements in genomic DNA isolated from total thymoyctes and splenocytes of WT, Vβ1^NT/+, or Vβ1^NT/NT mice. As anticipated, we found VβDJβ1.1, VβDJβ1.2, VβDJβ2.1, and VβDJβ2.2 rearrangements involving Vβ4, Vβ8, Vβ10, or Vβ14 segments in thymocytes and splenocytes of WT mice (Figure 3b, data not shown). We detected low levels, or failed to observe, VβDJβ1.1, VβDJβ1.2, VβDJβ2.1, and VβDJβ2.2 rearrangements involving Vβ4, Vβ8, Vβ10, or Vβ14 segments in thymocytes and splenocytes of Vβ1^NT/+ mice (Figure 3b, data not shown). We also conducted PCR analysis on serially diluted Vβ1^NT/NT thymocyte DNA to quantify the levels of VβDJβ2.1 and VβDJβ2.2 rearrangements involving Vβ10, Vβ16, or Vβ14. We found that Vβ10 segments rearranged at levels ~25-fold greater than Vβ16 or Vβ14 segments (Figure 3c). These data demonstrate that the significantly greater expression of Vβ10, as compared to Vβ16 or Vβ14, within cell surface TCRβ chains on Vβ1^NT/NTαβ T lineage cells is due to the differential regulation of rearrangements involving Vβ10 versus Vβ16 or Vβ14.

Since PCR based analyses of V(D)J recombination are semi-quantitative, we also generated panels of Vβ1^NT/+ and Vβ1^NT/NTαβ T cell hybridomas to quantify Vβ-to-DJβ rearrangements on a single cell basis. For this purpose, we conducted Southern blot analysis with a series of TCRβ locus probes on genomic DNA isolated from these clonal hybridomas. Of the 171 Vβ1^NT/+ hybridomas analyzed, nine (5.3%) contained Vβ rearrangements on the wild-type allele with three (1.8%) to DJβ1 complexes and six (3.5%) to DJβ2 complexes (Table 1). These data are consistent with the PCR and FACS analyses that revealed germline Vβ segments have rearranged and are expressed from wild-type alleles in Vβ1^NT/+αβ T lineage cells. Of the 228 Vβ1^NT/NT hybridomas analyzed, seven (3.1%) contained Vβ rearrangements to DJβ2 complexes on a single allele, all of which involved Vβ10 (Table 1). These data confirm that Vβ10 is the only germline Vβ segment that rearranges at an appreciable level to DJβ2 complexes in Vβ1^NT/NTαβ T cells. Importantly, this analysis also reveals that Vβ10-to-DJβ2 rearrangements occur on Vβ1^NT alleles in approximately 3% of Vβ1^NT/NT thymocytes and therefore are not rare recombination events.

Developmental Stage-Specific Transcription of Germline Vβ10 Segments on Vβ1^NT Alleles

The steady-state levels of germline transcripts are commonly used as a correlative measure of RAG accessibility. Although transcription through gene segments is not required for V(D)J recombination *per se*, the ability of transcriptional control elements to promote general chromatin accessibility and re-position nucleosomes appear critical for the RAG proteins to bind and cleave RSSs (18,19). To measure the steady-state levels of germline Vβ transcripts from Vβ1^NT alleles, we generated and analyzed Vβ1^NT/+Rag1^−/− and Vβ1^NT/NTRag1^−/−mice. The use of a Rag1^−/− background prevents the rearrangement of accessible germline Vβ segments. We conducted qPCR analysis of total RNA isolated from thymocytes of these mice using random hexamers and reverse-transcriptase to synthesize

cDNA. Primers located within the second exon of particular Vβ segments were used to amplify Vβ transcripts (Figure 4a), which were normalized to 18s RNA. As expected due to expression of the pre-assembled Vβ1DJβ1.4Cβ1 gene, we found high levels of Vβ1 transcripts in Vβ1$^{NT/+}$Rag1$^{-/-}$ and Vβ1$^{NT/NT}$Rag1$^{-/-}$ thymocytes (Figure 4b). We reproducibly detected germline Vβ transcripts involving only Vβ10 segments in Vβ1$^{NT/+}$Rag1$^{-/-}$ and Vβ1$^{NT/NT}$Rag1$^{-/-}$ thymocytes (Figure 4b). These data suggest that Vβ10 is the only germline Vβ segment transcribed at detectable levels on Vβ1^{NT} alleles in total thymocytes, mirroring our previous finding that Vβ10 is the predominant germline Vβ segment that rearranges on Vβ1^{NT} alleles.

To evaluate whether transcription of germline Vβ10 segments is influenced when Vβ1 segments participate in VβDJβ rearrangements, we generated and analyzed Vβ14$^{NT/+}$Rag1$^{-/-}$ and Vβ14$^{NT/NT}$Rag1$^{-/-}$ mice. The Vβ1 segment resides within the germline configuration on the Vβ14^{NT} allele. We conducted qPCR analysis of mRNA isolated from total thymocytes of these mice as described above. As expected due to expression of the pre-assembled Vβ14DJβ1.4Cβ1 gene, we found high levels of Vβ14 transcripts in Vβ14$^{NT/+}$Rag1$^{-/-}$ and Vβ14$^{NT/NT}$Rag1$^{-/-}$thymocytes (Figure 4c). However, we were unable to detect germline Vβ transcripts in Vβ14$^{NT/+}$Rag1$^{-/-}$ or Vβ14$^{NT/NT}$Rag1$^{-/-}$ thymocytes (Figure 4c). These data suggest that the participation of Vβ1 in VβDJβ rearrangements leads to increased transcription, and by extension RAG accessibility, of germline Vβ10 segments that reside immediately upstream of the assembled Vβ1DJβ exon.

We next sought to evaluate whether transcription of germline Vβ10 segments upstream of assembled Vβ1DJβ exons is maintained in naive αβ T cells. For this purpose, we used Vβ1$^{NT/NT}$ and Vβ14$^{NT/NT}$ mice to quantify germline Vβ transcripts in enriched splenic αβ T cells. We conducted qPCR analysis using the primers described above, as well as one primer located within the second exon and another primer located downstream of the RSS of particular Vβ segments (Figure 4d). Due to their locations, these second primer pairs can only amplify germline Vβ transcripts. As expected, we found rearranged, but not germline, transcripts involving Vβ1 and Vβ14 in Vβ1$^{NT/NT}$ and Vβ14$^{NT/NT}$ splenic αβ T cells, respectively (data not shown). We detected rearranged, but not germline, transcripts involving Vβ10 in Vβ1$^{NT/NT}$ splenic αβ T cells, and neither rearranged nor germline Vβ10 transcripts in Vβ14$^{NT/NT}$ cells (Figure 4e). These data suggest that germline Vβ segments are not transcribed on Vβ1^{NT} and Vβ14^{NT} alleles in peripheral αβ T cells. Importantly, this finding demonstrates that the transcription of germline Vβ10 segments on Vβ1^{NT} alleles is silenced in a developmental stage-specific manner during αβ T cell differentiation.

Developmentally regulated anti-sense transcripts have been found throughout intergenic regions of the IgH locus and suggested to function in suppression of D_H-to-J_H recombination and activation of V_H rearrangements (20–22). Thus, we decided to assay for the presence of anti-sense Vβ1 and Vβ10 transcripts in total thymocytes of Vβ1$^{NT/+}$Rag1$^{-/-}$ and Vβ1$^{NT/NT}$Rag1$^{-/-}$ mice. For this purpose, we conducted qPCR analysis of total RNA isolated from these cells using strand-specific primers and reverse-transcriptase to synthesize cDNA. Primers located within the second exon of Vβ1 or Vβ10 were used for qPCR amplification (Figure 5a). As expected, we detected sense transcripts involving rearranged Vβ1 and germline Vβ10 segments in Vβ1$^{NT/+}$Rag1$^{-/-}$ and Vβ1$^{NT/NT}$Rag1$^{-/-}$ thymocytes (Figure 5b). We detected anti-sense transcripts involving rearranged Vβ1 and germline Vβ10 segments in Vβ1$^{NT/+}$Rag1$^{-/-}$ and Vβ1$^{NT/NT}$Rag1$^{-/-}$ thymocytes (Figure 5c). Since germline Vβ10 segments are not transcribed in Vβ1$^{NT/NT}$αβ T cells (Figure 4e), these data indicate that developmentally regulated anti-sense transcription occurs through germline Vβ10 segments on Vβ1^{NT} alleles. Next, we conducted qPCR analysis with primer pairs to amplify potential sense or anti-sense transcripts involving sequences within the

Vβ10 promoter or immediately downstream of Vβ10 (Figure 5d). We observed sense transcripts involving sequences within the Vβ10 promoter and immediately downstream of Vβ10 (Figure 5e). We detected anti-sense transcripts involving sequences within the Vβ10 promoter, but not sequences immediately downstream of Vβ10 (Figure 5e). These data suggest that developmentally regulated anti-sense transcription does not occur throughout the entire Vβ10-Vβ1 intergenic region, but rather initiates within or very close to Vβ10 coding sequences. The potential function(s), if any, of this anti-sense germline transcription is unclear and could involve positive and/or negative regulation of Vβ10 accessibility and rearrangement.

CpG Methylation over Vβ10 Segments Correlates with Transcriptional Silencing

CpG methylation correlates with transcriptional silencing, can block RAG cleavage, and may render antigen receptor loci RAG inaccessible (16,23–27). Thus, we sought to determine whether differential CpG methylation of germline Vβ10 segments on Vβ1[NT] and Vβ14[NT] alleles correlated with their observed transcription and rearrangement patterns in thymocytes. For this purpose, we digested genomic DNA isolated from Vβ1[NT/NT] or Vβ1[NT/NT] total thymocytes with methyl-sensitive restriction enzymes. We then conducted qPCR using primer pairs that flank such restrictions sites within the Vβ10 promoter (site P) and the Vβ10 coding region (site C)(Figure 6a) to assess the percentage of cleavage, which correlates with the level of un-methylated CpG sites. Percent methylation was determined through dividing normalized digested Vβ10 amplicon values by normalized un-digested Vβ10 amplicon values. We found that the Vβ10 promoter (site P) and Vβ10 coding region (site C) were 20% methylated in Vβ1[NT/NT] thymocytes and 60–80% methylated in Vβ14[NT/NT] thymocytes (Figure 6b,c). As an independent means to assess CpG methylation, we conducted bisulfite sequence analysis of two other CpG sites (B1 and B2) within Vβ10 coding sequences (Figure 6a). Bisulfite sequencing showed that these Vβ10 coding sequences were 50% (site B1) and 13% (site B2) methylated in Vβ1[NT/NT] thymocytes and 88% methylated (sites B1 and B2) in Vβ14[NT/NT] thymocytes (Figure 6d). Unfortunately, we could not use either methyl-sensitive restriction enzymes or bisulfite sequencing to assay other CpG sites within the Vβ4-Vβ1 region of the TCRβ locus due to the high density of repetitive DNA elements. Regardless, these data reveal that increased CpG methylation of germline Vβ10 segments on Vβ14[NT] alleles correlates with their transcriptional and recombinational silencing.

We next sought to evaluate whether differential CpG methylation of Vβ10 segments on Vβ1[NT] alleles could account for the developmental stage-specific pattern of germline Vβ10 transcription. For this purpose, we analyzed genomic DNA isolated from Vβ1[NT/NT] splenic αβ T cells as outlined above. We found that sequences within the Vβ10 promoter (site P) and the Vβ10 coding region (site C) were 60–80% methylated in Vβ1[NT/NT] splenic αβ T cells (Figure 6e). These data indicate that the developmental stage-specific induction of CpG methylation over the Vβ10 promoter and coding region correlates with the transcriptional silencing of germline Vβ10 segments on Vβ1[NT/NT] alleles.

Repetitive DNA sequences can target silencing factors that promote CpG methlyation and function as boundaries between transcribed and silenced genetic loci (23,28). Thus, we evaluated the CpG methylation status of restriction sites (T1 and T2) among the Vβ16-Vβ10 intergenic repetitive DNA sequences (Figure 6a). We found that these sequences were 80% methylated in both Vβ1[NT/NT] and Vβ14[NT/NT] thymocytes, as well as in Vβ1[NT/NT] splenic αβ T cells (Figure 6b,c,e). These data indicate that CpG methylation of genomic DNA sequences within theVβ16-Vβ10 intergenic region marks the transition between transcribing Vβ10 segments and silent Vβ16 segments.

Histone Modifications over Vβ10 Segments Correlate with Transcriptional Activity

Since transcription and low CpG methylation are indicative of open chromatin, which is associated with histone H3 and H4 acetylation, we sought to determine whether differential histone acetylation over germline Vβ10 segments on Vβ1^{NT} and Vβ14^{NT} alleles correlates with their observed CpG methylation and transcription patterns. For this purpose, we conducted chromatin immunoprecipitation (ChIP) with anti-acetyl-H3 and anti-acetyl-H4 antibodies on mononucleosomes isolated from total thymocytes and splenic αβ T cells of Vβ1$^{NT/NT}$ mice. We found that acetylation of histone H3 and H4 were both high over germline Vβ10 segments and substantially lower over Vβ4, Vβ16, and intergenic sequences between Vβ16 and Vβ10 in thymocytes (Figure 7a,b). Histone H3 and H4 acetylation over Vβ1 was lower than over Vβ10 (Figure 7a,b), consistent with lower histone occupancy over Vβ1 due to the high level of transcription through the Vβ1DJβCβ1 gene. We found reduced levels of histone H3 and H4 acetylation over germline Vβ10 segments in splenic αβ T cells (Figure 7c). These data indicate that germline Vβ10 segments immediately upstream of the Vβ1DJβCβ1 gene reside within open and active chromatin, while Vβ4, Vβ16, and intergenic sequences between Vβ16 and Vβ10 reside within closed and silent chromatin.

Discussion

We have investigated whether Vβ-to-DJβ2 rearrangements can occur on alleles with assembled VβDJβCβ1 genes by analyzing αβ T lineage cells of mice containing the pre-assembled functional Vβ1^{NT} or Vβ14^{NT} gene. We found Vβ-to-DJβ2 rearrangements on Vβ1^{NT} alleles in ~3% of αβ T cells, while no Vβ-to-DJβ2 rearrangements were detectable on Vβ14^{NT} alleles. These data provide direct evidence that Vβ segments can rearrange to DJβ2 complexes over functional VβDJβCβ1 genes. In wild-type thymocytes, secondary Vβ rearrangements to DJβ2 complexes on alleles with assembled VβDJβCβ1 genes may occur at similar frequencies. Such Vβ-to-DJβ2 rearrangements on alleles with out-of-frame VβDJβCβ1 genes could account for or contribute to the ~1% of αβ T cells that exhibit TCRβ allelic inclusion (29–31). However, our experiments cannot rule out the possibility that Vβ-to-DJβ2 rearrangements on Vβ1^{NT} alleles arise from non-physiologic regulation of Vβ rearrangements. For example, the ability of the Vβ1^{NT} allele to bypass the necessity of assembling TCRβ genes through DNA double strand break (DSB) intermediates may prevent the activation of ATM dependent signals and chromatin modifications that suppress Vβ cleavage and transcription/accessibility (32,33). Our data also reveal that alleles with a functional Vβ14JβCβ1 gene do not allow Vβ-to-DJβ2 rearrangements, which likely would require developmental stage-specific TCRβ locus contraction by looping between Vβ segments and DJβ2 complexes (5). Thus, Vβ1^{NT} and Vβ14^{NT} may accelerate thymocyte development to an extent such that Vβ-to-DJβ2 rearrangements can occur across short distances on Vβ1^{NT} alleles, but not over large distances on Vβ14^{NT} alleles in DN cells.

Our study reveals that the position of germline Vβ segments relative to assembled in-frame VβDJβCβ1 genes influences their activity and overlaying chromatin structure. Vβ10 segments were transcribed, rearranged, and expressed in thymocytes on Vβ1^{NT}, but not Vβ14^{NT}, alleles. This Vβ14^{NT} allele-dependent silencing of Vβ10 correlated with increased CpG methylation and decreased histone acetylation over the Vβ10 promoter and coding region. Germline Vβ4 and Vβ16 segments upstream of Vβ10 were not transcribed, rearranged, or expressed at significant levels on Vβ1^{NT} or Vβ14^{NT} alleles, which correlated with low histone acetylation over Vβ4 and Vβ16. The activity and open chromatin structure of germline Vβ10 segments on Vβ1^{NT}, but not Vβ14^{NT}, alleles must be due to structural differences between these TCRβ loci imparted by the assembled VβDJβCβ1 genes. Based upon other's conclusions (34), one possibility is that the Vβ1^{NT} gene brings Vβ10, but neither Vβ4 nor Vβ16, into the TCRβ enhancer (Eβ) regulatory domain. Similar to the Vβ1^{NT} allele, the rearrangement and transcription of Vβ10, but not Vβ4 or Vβ16, is

substantially elevated on a TCRβ allele with a 475 kb deletion that places Vβ10 just upstream of Cβ1 (34). Since Eβ affects transcription and chromatin accessibility over a limited region of the TCRβ locus from Dβ1 to just 3′ of Eβ (35), it was concluded that this 475 kb deletion brings Vβ10 into the Eβ regulatory domain but not Vβ4 and Vβ16, which are located 13.5 kb upstream (34). Yet, since enhancer activity can be restricted by promoter/enhancer interactions and boundary elements (36), another possibility is that interaction between Eβ and the Vβ10 promoter and/or boundary elements in the Vβ4/Vβ16--Vβ10 intergenic region restrict Eβ activity to Vβ10. Such mechanisms also could explain the normal rearrangement and transcription of a Vβ13 segment inserted just upstream of Dβ1 (37), since Eβ and the Dβ1 promoter (pDβ1) form a holoenzyme complex and both DNA repeats and other putative boundary elements reside just upstream of pDβ1 (3,9,38).

Our observations that Vβ10, but not Vβ4 or Vβ16, segments on the Vβ1[NT] allele reside within active chromatin in thymocytes provide novel insights into mechanisms that regulate Vβ rearrangements. In DP thymocytes, TCRβ locus de-contraction and epigenetic silencing of Vβ chromatin likely function together to inhibit primary Vβ rearrangements on DJβ-rearranged alleles (5,6). Additional mechanism(s) have been proposed to prevent secondary Vβ rearrangements over VβDJβCβ1 genes in DP thymocytes based upon data that germline Vβ segments located upstream of functional VβDJβCβ genes, which do not rearrange in DP cells, can exhibit transcription and/or histone acetylation in mature αβ T cells (11,39). The finding that germline Vβ10 segments on the Vβ1[NT] allele are transcribed and contain high levels of histone H3 and H4 acetylation in total thymocytes provides direct evidence that epigenetic silencing of Vβ chromatin cannot inhibit all secondary Vβ rearrangements in DP cells. Thus, secondary Vβ rearrangements may be regulated by developmental stage-specific factors (11), which control RAG binding to Vβ or 5′Dβ RSSs, synapsis between Vβ segments and DJβ complexes, and/or RAG accessibility independent of transcription and histone H3 acetylation. Considering that Vβ and Dβ2 DNA ends are detectable in DP thymocytes of wild-type mice (8), such mechanisms may actively suppress but not completely prevent the rearrangement of all upstream Vβ segments over VβDJβCβ1 genes in DP cells. In this context, some fraction of the Vβ10-to-DJβ2 rearrangements on Vβ1[NT] alleles may occur in DP thymocytes. Similar to previous observations in mature αβ T cells (11), our data reveal that germline transcription and chromatin structure of Vβ segments located upstream of functional VβDJβCβ1 genes are not uniformly regulated in total thymocytes. These differences could be due to the location of Vβs relative to assembled VβDJβCβ genes, intrinsic properties of Vβ promoters (40), the proximity of Vβ promoters to Eβ (34), and/or the density of flanking DNA repeat elements (20); all of which also could account for Dβ-Jβ transcription throughout thymocyte development.

Developmental stage-specific regulation of CpG methylation over Dβ-Jβ-Cβ sequences correlates with germline transcription and rearrangement of Dβ-Jβ segments and expression of assembled VβDJβCβ genes (35,41–43). Our data reveals that developmental stage-specific silencing of germline Vβ10 transcription coincides with increased CpG methylation of the Vβ10 promoter and coding region. In thymocytes, germline Vβ10 segments on the Vβ1[NT] allele are transcribed, exhibit low CpG methylation, and reside within highly acetylated chromatin. Germline Vβ10 transcription is silenced in αβ T cells, correlating with a four-fold increase in CpG methylation and a 50-fold reduction in histone H3 acetylation. The mechanisms by which this developmental stage-specific CpG methylation occurs and the potential physiologic relevance of this phenomenon remain to be determined. CpG methylation can be targeted by nearby LINE promoters and RNA interference pathways activated by sense and anti-sense transcription (44). Such mechanisms may direct CpG methylation of germline Vβ10 segments on the Vβ1[NT] allele since partial LINE elements reside within the Vβ4/Vβ16-Vβ10 intergenic region and germline Vβ10 sense and anti-sense transcription precedes CpG methylation. Recent evidence has demonstrated unequivocally

that TCRβ revision through Vβ-to-DJβ2 rearrangements over functional VβDJβCβ1 genes in mature αβ T cells contributes to the peripheral tolerance of endogenous antigens (45). Yet, dominant cell autonomous peripheral tolerance mechanisms, such as those mediated by regulatory T cells, may require maintained expression of auto-reactive αβ TCRs (46). Since CpG methylation can prevent V(D)J recombination through forming RAG inaccessible chromatin or blocking RAG cleavage by recruiting methyl-CpG binding proteins (24), the induction and maintenance of CpG methylation over germline Vβ segments upstream of functional VβDJβCβ1 genes in mature αβ T cells may contribute to the effectiveness of peripheral tolerance.

Supplementary Material

Refer to Web version on PubMed Central for supplementary material.

Acknowledgments

References

1. von Boehmer H. Selection of the T-cell repertoire: receptor-controlled checkpoints in T-cell development. Adv Immunol. 2004; 84:201–238. [PubMed: 15246254]

2. Jackson AM, Krangel MS. Turning T-cell receptor beta recombination on and off: more questions than answers. Immunol Rev. 2006; 209:129–141. [PubMed: 16448539]

3. Glusman G, Rowen L, Lee I, Boysen C, Roach JC, Smit AF, Wang K, Koop BF, Hood L. Comparative genomics of the human and mouse T cell receptor loci. Immunity. 2001; 15:337–349. [PubMed: 11567625]

4. Khor B, Sleckman BP. Intra- and inter-allelic ordering of T cell receptor beta chain gene assembly. Eur J Immunol. 2005; 35:964–970. [PubMed: 15719363]

5. Skok JA, Gisler R, Novatchkova M, Farmer D, de Laat W, Busslinger M. Reversible contraction by looping of the Tcra and Tcrb loci in rearranging thymocytes. Nat Immunol. 2007; 8:378–387. [PubMed: 17334367]

6. Tripathi R, Jackson A, Krangel MS. A change in the structure of Vbeta chromatin associated with TCR beta allelic exclusion. J Immunol. 2002; 168:2316–2324. [PubMed: 11859121]

7. Senoo M, Shinkai Y. Regulation of Vbeta germline transcription in RAG-deficient mice by the CD3epsilon-mediated signals: implication of Vbeta transcriptional regulation in TCR beta allelic exclusion. Int Immunol. 1998; 10:553–560. [PubMed: 9645603]

8. Jackson A, Kondilis HD, Khor B, Sleckman BP, Krangel MS. Regulation of T cell receptor beta allelic exclusion at a level beyond accessibility. Nat Immunol. 2005; 6:189–197. [PubMed: 15640803]

9. Chattopadhyay S, Whitehurst CE, Schwenk F, Chen J. Biochemical and functional analyses of chromatin changes at the TCR- beta gene locus during CD4-CD8-to CD4+CD8+ thymocyte differentiation. J Immunol. 1998; 160:1256–1267. [PubMed: 9570542]

10. Wang L, Senoo M, Habu S. Differential regulation between gene expression and histone H3 acetylation in the variable regions of the TCRbeta locus. Biochem Biophys Res Commun. 2002; 298:420–426. [PubMed: 12413958]

11. Jackson AM, Krangel MS. Allele-specific regulation of TCR beta variable gene segment chromatin structure. J Immunol. 2005; 175:5186–5191. [PubMed: 16210623]

12. Serwold T, Hochedlinger K, Inlay MA, Jaenisch R, Weissman IL. Early TCR expression and aberrant T cell development in mice with endogenous prerearranged T cell receptor genes. J Immunol. 2007; 179:928–938. [PubMed: 17617584]

13. Hochedlinger K, Jaenisch R. Monoclonal mice generated by nuclear transfer from mature B and T donor cells. Nature. 2002; 415:1035–1038. [PubMed: 11875572]

14. Carpenter AC, Yang-Iott KS, Chao LH, Nuskey B, Whitlow S, Alt FW, Bassing CH. Assembled DJ beta complexes influence TCR beta chain selection and peripheral V beta repertoire. J Immunol. 2009; 182:5586–5595. [PubMed: 19380806]

15. Allman D, Sambandam A, Kim S, Miller JP, Pagan A, Well D, Meraz A, Bhandoola A. Thymopoiesis independent of common lymphoid progenitors. Nat Immunol. 2003; 4:168–174. [PubMed: 12514733]

16. Godfrey DI, Kennedy J, Mombaerts P, Tonegawa S, Zlotnik A. Onset of TCR-beta gene rearrangement and role of TCR-beta expression during CD3-CD4-CD8-thymocyte differentiation. J Immunol. 1994; 152:4783–4792. [PubMed: 7513723]

17. Steinel NC, Brady BL, Carpenter AC, Yang-Iott KS, Bassing CH. Posttranscriptional silencing of VbDJbCb genes contributes to TCRb allelic exclusion in mammalian lymphocytes. J Immunol. 2010 In Press.

18. Sikes ML, Meade A, Tripathi R, Krangel MS, Oltz EM. Regulation of V(D)J recombination: a dominant role for promoter positioning in gene segment accessibility. Proc Natl Acad Sci U S A. 2002; 99:12309–12314. [PubMed: 12196630]

19. Abarrategui I, Krangel MS. Noncoding transcription controls downstream promoters to regulate T-cell receptor alpha recombination. Embo J. 2007; 26:4380–4390. [PubMed: 17882258]

20. Chakraborty T, Chowdhury D, Keyes A, Jani A, Subrahmanyam R, Ivanova I, Sen R. Repeat organization and epigenetic regulation of the DH-Cmu domain of the immunoglobulin heavy-chain gene locus. Mol Cell. 2007; 27:842–850. [PubMed: 17803947]

21. Bolland DJ, Wood AL, Afshar R, Featherstone K, Oltz EM, Corcoran AE. Antisense intergenic transcription precedes Igh D-to-J recombination and is controlled by the intronic enhancer Emu. Mol Cell Biol. 2007; 27:5523–5533. [PubMed: 17526723]

22. Bolland DJ, Wood AL, Johnston CM, Bunting SF, Morgan G, Chakalova L, Fraser PJ, Corcoran AE. Antisense intergenic transcription in V(D)J recombination. Nat Immunol. 2004; 5:630–637. [PubMed: 15107847]

23. Bird A. DNA methylation patterns and epigenetic memory. Genes Dev. 2002; 16:6–21. [PubMed: 11782440]

24. Nakase H, Takahama Y, Akamatsu Y. Effect of CpG methylation on RAG1/RAG2 reactivity: implications of direct and indirect mechanisms for controlling V(D)J cleavage. EMBO Rep. 2003; 4:774–780. [PubMed: 12897800]

25. Mostoslavsky R, Singh N, Kirillov A, Pelanda R, Cedar H, Chess A, Bergman Y. Kappa chain monoallelic demethylation and the establishment of allelic exclusion. Genes Dev. 1998; 12:1801–1811. [PubMed: 9637682]

26. Osipovich O, Milley R, Meade A, Tachibana M, Shinkai Y, Krangel MS, Oltz EM. Targeted inhibition of V(D)J recombination by a histone methyltransferase. Nat Immunol. 2004; 5:309–316. [PubMed: 14985714]

27. Hsieh CL, Lieber MR. CpG methylated minichromosomes become inaccessible for V(D)J recombination after undergoing replication. Embo J. 1992; 11:315–325. [PubMed: 1371250]

28. Grewal SI, Jia S. Heterochromatin revisited. Nat Rev Genet. 2007; 8:35–46. [PubMed: 17173056]

29. Davodeau F, Peyrat MA, Houde I, Hallet MM, De Libero G, Vie H, Bonneville M. Surface expression of two distinct functional antigen receptors on human gamma delta T cells. Science. 1993; 260:1800–1802. [PubMed: 8390096]

30. Padovan E, Casorati G, Dellabona P, Meyer S, Brockhaus M, Lanzavecchia A. Expression of two T cell receptor alpha chains: dual receptor T cells. Science. 1993; 262:422–424. [PubMed: 8211163]

31. Balomenos D, Balderas RS, Mulvany KP, Kaye J, Kono DH, Theofilopoulos AN. Incomplete T cell receptor V beta allelic exclusion and dual V beta-expressing cells. J Immunol. 1995; 155:3308–3312. [PubMed: 7561023]

32. Shanbhag NM I, Rafalska-Metcalf U, Balane-Bolivar C, Janicki SM, Greenberg RA. ATM-dependent chromatin changes silence transcription in cis to DNA double-strand breaks. Cell. 2010; 141:970–981. [PubMed: 20550933]

33. Hewitt SL, Yin B, Ji Y, Chaumeil J, Marszalek K, Tenthorey J, Salvagiotto G, Steinel N, Ramsey LB, Ghysdael J, Farrar MA, Sleckman BP, Schatz DG, Busslinger M, Bassing CH, Skok JA. RAG-1 and ATM coordinate monoallelic recombination and nuclear positioning of immunoglobulin loci. Nat Immunol. 2009; 10:655–664. [PubMed: 19448632]

34. Senoo M, Wang L, Suzuki D, Takeda N, Shinkai Y, Habu S. Increase of TCR V beta accessibility within E beta regulatory region influences its recombination frequency but not allelic exclusion. J Immunol. 2003; 171:829–835. [PubMed: 12847251]

35. Mathieu N, Hempel WM, Spicuglia S, Verthuy C, Ferrier P. Chromatin remodeling by the T cell receptor (TCR)-beta gene enhancer during early T cell development: Implications for the control of TCR-beta locus recombination. J Exp Med. 2000; 192:625–636. [PubMed: 10974029]

36. Blackwood EM, Kadonaga JT. Going the distance: a current view of enhancer action. Science. 1998; 281:61–63.

37. Sieh P, Chen J. Distinct control of the frequency and allelic exclusion of the V beta gene rearrangement at the TCR beta locus. J Immunol. 2001; 167:2121–2129. [PubMed: 11489996]

38. Oestreich KJ, Cobb RM, Pierce S, Chen J, Ferrier P, Oltz EM. Regulation of TCRbeta gene assembly by a promoter/enhancer holocomplex. Immunity. 2006; 24:381–391. [PubMed: 16618597]

39. Jia J, Kondo M, Zhuang Y. Germline transcription from T-cell receptor Vbeta gene is uncoupled from allelic exclusion. Embo J. 2007; 26:2387–2399. [PubMed: 17410206]

40. Chen F, Rowen L, Hood L, Rothenberg EV. Differential transcriptional regulation of individual TCR V beta segments before gene rearrangement. J Immunol. 2001; 166:1771–1780. [PubMed: 11160223]

41. Sakamoto S, Mathieson BJ, Komschlies KL, Bhat NK, Young HA. The methylation state of the T cell antigen receptor beta chain gene in subpopulations of mouse thymocytes. Eur J Immunol. 1989; 19:873–879. [PubMed: 2525476]

42. Hozumi K, Kobori A, Sato T, Nishimura T, Habu S. Transcription and demethylation of TCR beta gene initiate prior to the gene rearrangement in c-kit+ thymocytes with CD3 expression: evidence of T cell commitment in the thymus. Int Immunol. 1996; 8:1473–1481. [PubMed: 8921426]

43. Whitehurst CE, Schlissel MS, Chen J. Deletion of germline promoter PD beta 1 from the TCR beta locus causes hypermethylation that impairs D beta 1 recombination by multiple mechanisms. Immunity. 2000; 13:703–714. [PubMed: 11114382]

44. Chen T, Li E. Structure and function of eukaryotic DNA methyltransferases. Curr Top Dev Biol. 2004; 60:55–89. [PubMed: 15094296]

45. Hale JS, Ames KT, Boursalian TE, Fink PJ. Cutting Edge: Rag deletion in peripheral T cells blocks TCR revision. J Immunol. 2010; 184:5964–5968. [PubMed: 20435935]

46. Wing K, Sakaguchi S. Regulatory T cells exert checks and balances on self tolerance and autoimmunity. Nat Immunol. 2010; 11:7–13. [PubMed: 20016504]
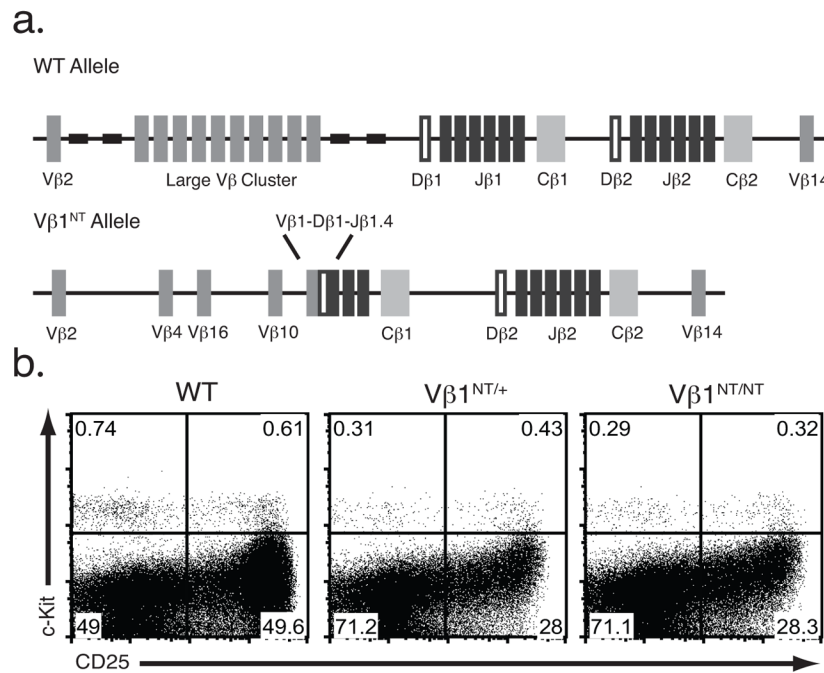
a.

WT Allele

Vβ2   Large Vβ Cluster   Dβ1   Jβ1   Cβ1   Dβ2   Jβ2   Cβ2   Vβ14

Vβ1^NT Allele   Vβ1-Dβ1-Jβ1.4

Vβ2   Vβ4 Vβ16   Vβ10   Cβ1   Dβ2   Jβ2   Cβ2   Vβ14

b.

Figure 1. Pre-assembled Functional Vβ1DJβ1.4Cβ1 Genes Accelerate Early Thymocyte Development
(a) Genomic organization of the wild-type and Vβ1^NT TCRβ alleles. Shown are schematic representations of the WT and Vβ1^NT alleles depicting the relative locations of the germline Vβ, Dβ, Jβ, and Cβ gene segments and the assembled Vβ1DJβ1.4 exon. The trypsinogen genes residing between the Vβ cluster and Vβ2 and Dβ1 are represented by black boxes. (b) FACS analyses of early thymocyte development in WT, Vβ1^NT/+, and Vβ1^NT/NT mice. Shown are representative plots of anti-ckit and anti-CD25 stains conducted on lineage negative thymocytes. The percentages of total events within each quadrant are indicated.
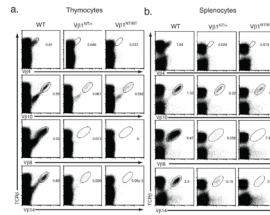
Figure 2. Vβ10 is the Predominant Germline Vβ Segment Expressed from Vβ1^{NT} Alleles
Shown are representative FACS analyses of (a) thymocytes and (b) splenocytes isolated from WT, Vβ1$^{NT/+}$, or Vβ1$^{NT/NT}$ mice. Cells were stained with anti-Cβ and either anti-Vβ4, anti-Vβ10, anti-Vβ8, or anti-Vβ14. The percentages of Cβ$^+$ cells expressing each Vβ within the circle gates are indicated. These data are representative of those obtained from the same experiments performed three independent times, each time on one mouse of each genotype.
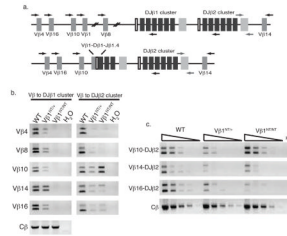
Figure 3. Vβ10 is the Predominant Germline Vβ Segment Rearranged on Vβ1^{NT} Alleles
(a) PCR strategy for amplification of Vβ-to-DJβ1 and Vβ-to-DJβ2 rearrangements. Shown are schematic representations of the WT and Vβ1^{NT} alleles depicting the relative locations of Vβ, Dβ, Jβ, and Cβ gene segments and the assembled Vβ1DJβ1.4 exon, as well as the Vβ specific primers, the primers located just downstream of Jβ1.2 or Jβ2.2, and the Cβ2 primers. (b) PCR analysis of potential Vβ-to-DJβ1 and Vβ-to-DJβ2 rearrangements. Shown are representative PCR amplifications of VβDJβ1.1, VβDJβ1.2, VβDJβ2.1, and VβDJβ2.1 rearrangements for the indicated Vβ segments conducted on genomic DNA isolated from thymocytes of WT, Vβ1$^{NT/+}$, or Vβ1$^{NT/NT}$ mice. Also shown is a representative PCR amplification of Cβ2 as a control for DNA content. These data are representative of those obtained from the same experiments performed three independent times, each time on one mouse of each genotype. (c) Semi-quantitative PCR analysis of Vβ-to-DJβ2 rearrangements. Shown are representative PCR amplifications of Vβ rearrangements to DJβ2.1/DJβ2.2 complexes for the indicated Vβ segments using serial 1:5 dilutions of DNA isolated from WT, Vβ1$^{NT/+}$, or Vβ1$^{NT/NT}$ mice thymocytes. Also shown is a representative PCR amplification of Cβ2 as a control for DNA content.
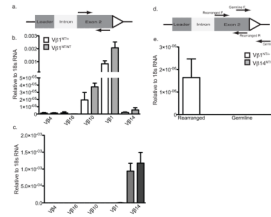
Figure 4. Vβ10 is the Predominant Germline Vβ Segment Transcribed on Vβ1^{NT} Alleles
(a) qPCR strategy for amplification of Vβ transcripts. Shown is the organization of a
germline Vβ segment indicating the relative positions of the leader exon, intron, exon 2, and
RSS (open triangle). The relative locations of the forward (RT F) and reverse primers (RT
R) used in qPCR reactions also are indicated. (b–c) qPCR analysis of germline Vβ
transcripts. Shown are data obtained from three independent qPCR assays for the indicated
Vβ segments conducted on total RNA isolated from thymocytes of (b) Vβ1$^{NT/+}$Rag1$^{-/-}$
(white) and Vβ1$^{NT/NT}$Rag1$^{-/-}$ (grey) mice or (c) Vβ14$^{NT/+}$Rag1$^{-/-}$ (dark grey) and
Vβ14$^{NT/NT}$Rag1$^{-/-}$ (black) mice. Transcripts were normalized to 18s RNA. Error bars are
standard error. (d) qPCR strategy for amplification of germline or rearranged Vβ transcripts.
Shown is the organization of a germline Vβ segment indicating the relative positions of the
leader exon, intron, exon 2, and RSS (open triangle). The relative locations of the forward
(F) and reverse primers (R) used in qPCR reactions for the amplification of rearranged or
germline Vβ transcripts also are indicated. (e) qPCR analysis of germline or rearranged Vβ
transcripts. Shown are data obtained from three independent qPCR assays for Vβ10
segments conducted on total RNA isolated from splenocytes of Vβ1$^{NT/NT}$ (white) or
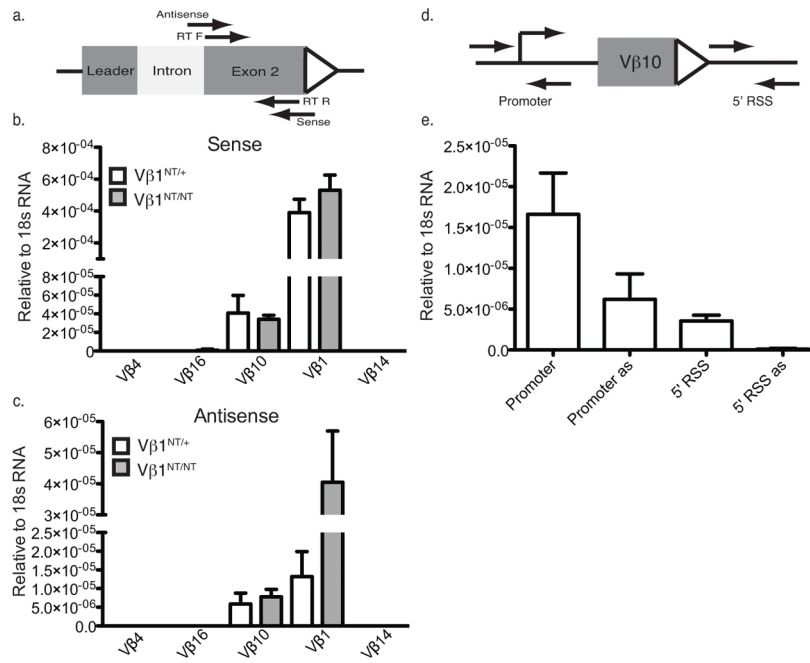Vβ14$^{NT/NT}$ (grey) mice. Transcripts were normalized to 18s RNA. Error bars are standard
error.

Figure 5. Sense and Anti-Sense Transcription of Germline Vβ10 Segments on Vβ1^NT Alleles
(a) qPCR strategy for amplification of strand-specific Vβ transcripts. Shown is the organization of a germline Vβ segment indicating the relative positions of the leader exon, intron, exon 2, and RSS (open triangle). The relative locations of the anti-sense and sense primers used to synthesize cDNA, and the forward (RT F) and reverse primers (RT R) used in qPCR reactions. (b–c) qPCR analysis of (b) sense and (c) anti-sense germline Vβ transcripts. Shown are data obtained from three independent qPCR assays for the indicated Vβ segments conducted on total RNA isolated from thymocytes of Vβ1^NT/+Rag1^−/− (white) or Vβ1^NT/NTRag1^−/−(grey) mice. Transcripts were normalized to 18s RNA. Error bars are standard error. (d) qPCR strategy for amplification of strand-specific transcripts involving sequences within the Vβ10 promoter or downstream of the Vβ10 RSS. Shown is the organization of a germline Vβ segment indicating the relative positions of the promoter (arrow), Vβ coding region, and RSS (open triangle). The relative locations of the forward and reverse primers used in qPCR reactions. The sense and anti-sense primers are not shown, but were located just upstream or downstream of the forward and reverse primers. (e) qPCR analysis of sense or anti-sense transcripts involving sequences within the Vβ10 promoter or downstream of the Vβ10 RSS. Shown are data obtained from three independent qPCR assays conducted on total RNA isolated from thymocytes of Vβ1^NT/NTRag1^−/− mice. Transcripts were normalized to 18s RNA. Error bars are standard error.
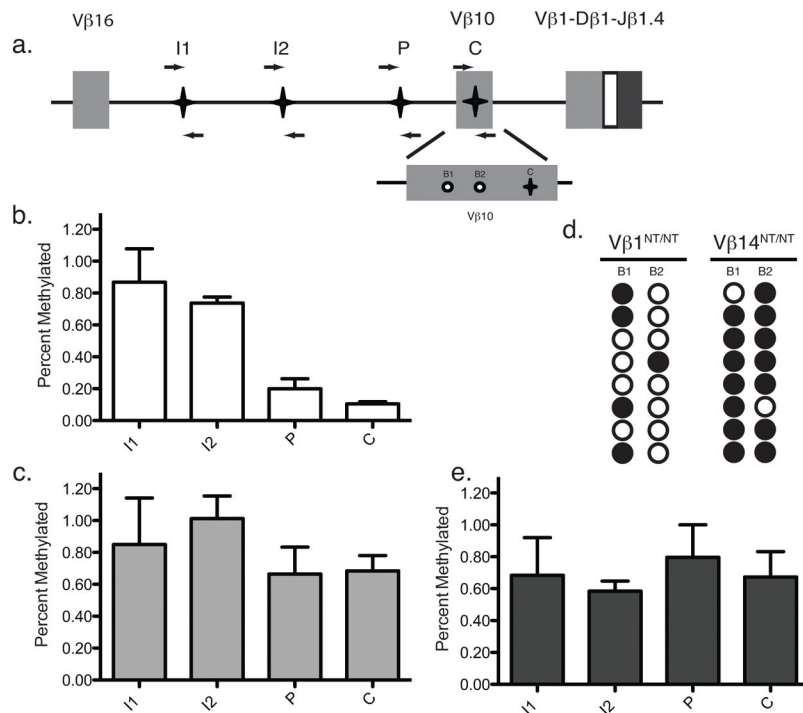
Figure 6. Developmental Stage-Specific and Position-Dependent CpG Methylation of Vβ10 Segments and Upstream Sequences on Vβ1NT and Vβ14NT Alleles
(a) Genomic organization of the Vβ16 and Vβ10 gene segments and the Vβ1DJβ1.4Cβ1 gene on the Vβ1NT allele. The location of the primers and the restriction sites within the Vβ16-Vβ10 intergenic region (sites I1 and I2), the Vβ10 promoter (site P), and the Vβ10 coding region (site C) used to assess CpG methylation by methyl-sensitive restriction enzyme digest are indicated. The location of the CpG sites (B1 and B2) assayed by bisulfite sequencing also are indicated. (b–c) CpG methylation status of Vβ10 segments and upstream sequences on Vβ1NT and Vβ14NT alleles in total thymocytes. Shown are data obtained from three independent restriction enzyme digest experiments conducted on genomic DNA isolated from (b) Vβ1NT/NTRag1−/− thymocytes or (c) Vβ14NT/NTRag1−/− thymocytes. Error bars are standard error. Differences in CpG methylation are significant between Vβ1NT/NTRag1−/− and Vβ14NT/NTRag1−/− thymocytes at sites P (p=0.04) and C (p=0.0002). (d) CpG methylation status of Vβ10 segments on Vβ1NT and Vβ14NT alleles in total thymocytes. Shown are data obtained from three independent bisulfite sequence experiments conducted on genomic DNA isolated from Vβ1NT/NTRag1−/− thymocytes or Vβ14NT/NTRag1−/−thymocytes. Filled circles indicate methylated CpG residues. (e) CpG methylation status of Vβ10 segments and upstream sequences on Vβ1NT alleles in splenic T cells. Shown are data obtained from three independent restriction enzyme digest experiments conducted on genomic DNA isolated from Vβ1NT/NT splenocytes. Error bars are standard error. Differences in CpG methylation are statistically significant between Vβ1NT/NTRag1−/− thymocytes and Vβ1NT/NT splenocytes at sites P (p=0.02) and C (p=0.003).
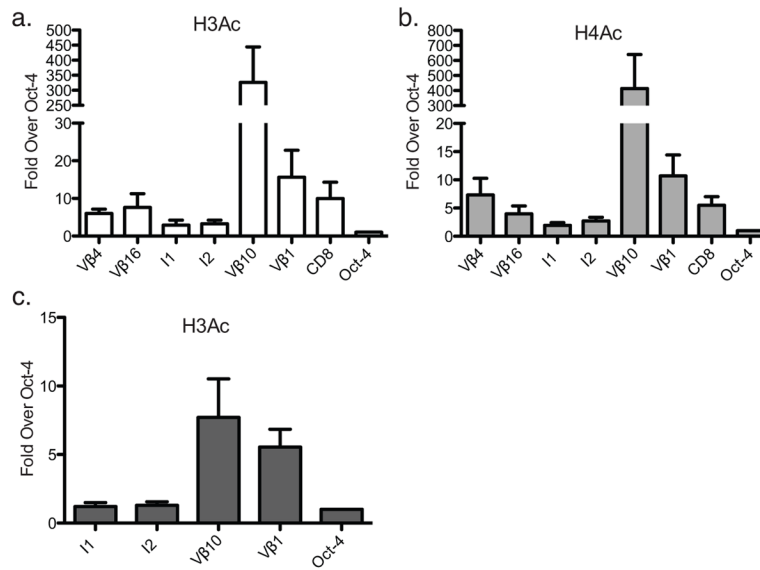
Figure 7. Developmental Stage-Specific and Position-Dependent Histone Modifications over Vβ10 Segments and Flanking Sequences on Vβ1^{NT} Alleles
(a–b) Histone modifications over Vβ10 segments and flanking sequences on Vβ1^{NT} alleles in total thymocytes. Shown are data obtained from three independent ChIP experiments for (a) anti-acetyl-H3 or (b) anti-acetyl-H4 conducted on Vβ1$^{NT/NT}$ thymocytes. Error bars are standard error. (c) Histone modifications over Vβ10 segments and flanking sequences on Vβ1^{NT} alleles in splenic T cells. Shown are data obtained from three independent ChIP experiments for anti-acetyl-H3 conductd on Vβ1$^{NT/NT}$ splenic T cells. Error bars are standard error.

Table I

Analysis of Vβ rearrangements in Vβ1[NT/+] and Vβ1[NT/NT]αβ T cell hybridomas

Southern blot analysis using a series of TCRβ locus probes was used to quantify TCRβ gene rearrangements on wild-type and Vβ1[NT] alleles in panels of Vβ1[NT/+] and Vβ1[NT/NT]αβ T cell hybridomas. All Vβ-to-DJβ2 rearrangements in Vβ1[NT/NT] cells involved Vβ10 segments.

	Number	VDJ Rearrangement			DJβ1 to DJβ2
		Total	VDJβ1	VDJβ2	
Vβ1[NT/+]					
Panel 937	80	5	2	3	21
Panel 943	91	4	1	3	25
Vβ1[NT/NT]					
Panel 934	93	4	-	4	-
Panel 612	135	3	-	3	-
Vβ1[NT/+]	171	5.3%	1.8%	3.5%	26.9%
Vβ1[NT/NT]	228	3.1%	-	3.1%	-